TECHNICAL TRANSACTIONS 4/2019
MECHANICS
DOI: 10.4467/2353737XCT.19.049.10361
SUBMISSION OF THE FINAL VERSION: 30/03/2019

Adrian Kozień orcid.org/0000-0001-5405-3608
adrian.kozien@pk.edu.pl
Faculty of Mechanical Engineering, Cracow University of Technology

The development and verification of a dynamic model of the Kawasaki RS010L industrial robot

Opracowanie oraz weryfikacja modelu dynamiki robota przemysłowego Kawasaki RS010L

Abstract

This article presents an attempt to develop a simplified dynamic model of the Kawasaki RS010L industrial robot using the Matlab mathematical environment. This is a six-axis robot which, due to its light weight and high movement ability, is used for a wide range of tasks, such as palletising and assembling objects. It was assumed that all links are stiff and the robot's wrist is a concentrated mass located at the end of the third arm. In addition, the axes are controlled independently of each other in this model. Essential parameters were identified using a real robot and the correctness of the developed model was verified.

Keywords: robot dynamics, dynamics model of robot, Kawasaki RS010L

Streszczenie

W niniejszym artykule podjęto próbę utworzenia w środowisku matematycznym Matlab uproszczonego modelu dynamiki przemysłowego robota Kawasaki RS010L. Jest to 6-osiowy robot, który dzięki małej wadze oraz dużym zdolnościom ruchowym jest stosowany do szerokiego spektrum zadań, takich jak paletyzacja czy montaż obiektów. Założono, że człony są sztywne, a kiść robota jest skupioną masą na końcu trzeciego ramienia. Przyjęto również, że sterowanie osiami robota odbywa się w sposób niezależny. Ponadto, korzystając z rzeczywistego obiektu, dokonano identyfikacji niezbędnych parametrów oraz zweryfikowano poprawność utworzonego modelu.

Słowa kluczowe: dynamika robotów, model dynamiki robota, Kawasaki RS010L

1. Introduction

Robot dynamics is a wide branch of mechanics which deals with the study of dependencies between motion and the forces and moments $\boldsymbol{\tau}$ which cause this motion. Robot motion is represented by a set of three variables in kinematic links: displacement $\boldsymbol{q}$, velocity $\dot{\boldsymbol{q}}$ and acceleration $\ddot{\boldsymbol{q}}$ [13]. The development of equations describing dependencies between motion and forces and moments allows us to test control strategies and motion planning techniques without using a physically available system.

Previous works on the dynamics of robots [5, 6] have typically been concerned with the determination of a mathematical model of an industrial anthropomorphic robot. More recent works focus not only on determining mathematical relations but also on the verification of received equations. The authors in [12] prepared a dynamic model of a two degrees-of-freedom (2 DOF) robot and simulated it using SIMNOM software. Furthermore, a prototype was made to assess its correctness. The total error of the trajectory for the first joint did not exceed 0.6 degrees, which can be considered to be a satisfying result. This procedure is often quite expensive and time-consuming. However, thanks to CAD program, with which the prototype was built, it is possible to identify the exact value of parameters characterising each component, such as dimensions, mass and inertia. In the case of large objects (usually complicated in assembly), the solution to this problem of identifying the exact values of these parameters is quite different. This means that many parameters can be read from specifications or CAD models provided by manufacturers. However, due to the company's strategy to maintain secrecy, not all of the information has been published, which was challenging for many scientists. Atkeson et al. [2] performed the estimation of the dynamic parameters using the least square method. In work [4], the authors attained a dynamic model of the SCARA robot from experimental data using the weighted least squares method. It has recently been discovered that heuristic algorithms are a useful tool for identifying robot parameters. A genetic algorithm was proposed to identify the parameters of the PUMA 560 robot [15]. A few years later, an improved genetic algorithm was introduced to obtain the model of space robot [10]. However, while dealing with complex and large-scale parameter identification problems, the genetic algorithm would be stuck on the local optimum. Therefore, the artificial bee colony algorithm (ABC) was proposed by Karaboga in 2005 [6] and it was successfully applied to various kinds of problem, such as parameter identification of the aerial robot [8]. This is because previous optimisation algorithms conduct only one search operation in each iteration, while the ABC algorithm can conduct both a local search and a global search in each iteration, thus the probability of finding optimal parameters is significantly increased. The ABC algorithm was introduced to examine the missing parameters of the 6-DOF ER-16 industrial robot [10].

In this paper, a simplified dynamic model of the Kawasaki RS010L industrial robot using the Matlab mathematical environment was made. In addition, using the data from the manufacturer and the physically available robot, identification of the necessary parameters and verification of the previously created model were carried out.

2. Dynamic modelling

There are two basic types of dynamics tasks: direct and inverse. In the first task, forces and moments on the motors are provided and the goal is to find the course of changes in the values of the robot's motion parameters over time. This procedure is useful in the case of robot motion simulation. The inverse dynamic task can be used to control the robot because the input value is the robot's trajectory and the output value is the course of changes in the value of the forces and moments on the motors. Creating the model is the first step in considering tasks such as dynamic analysis, optimisation and control. Having a real object allows us to check the correctness of the built model. After verification, this model is a perfect tool to solve more complex problems [14]. The method of the building and verification of a mathematical model of an industrial robot is presented below.

Firstly, there is a need to create robot motion equations. Two methods can be used for this purpose (assuming fully rigid elements) [6, 11]:

Newton–Euler – which describes the dynamics of each link,

Lagrange – which describes the dynamics of the whole robot using kinetic and potential energy.

The first of these methods considers each link separately using linear and angular motion equations. It is obvious that if links are connected, there are linkages between them that result from forces and moments. A "forward–backward recursion" method enables the defining of expressions, which helps to obtain a complete description of the manipulator ? By contrast, the second procedure considers the robot as a whole and considers energy dependences by using generalised coordinates (in this case: $\boldsymbol{q}$). Due to these internal links, forces of reaction are not considered. Therefore, the way to formulate equations is quite fast and yields the same result as the first method. The only disadvantage is that it doesn't provide complete information about the examined object. The final equations can be written as follows (1):

$$\mathbf{B}(\boldsymbol{q})\ddot{\boldsymbol{q}}+\mathbf{C}(\boldsymbol{q},\dot{\boldsymbol{q}})+\mathbf{g}(\boldsymbol{q})=\boldsymbol{\tau} \tag{1}$$

where:

B – matrix of inertia,

C – matrix of centrifugal and Coriolis forces,

g – matrix of gravitational forces,

$\boldsymbol{\tau}$ – vector of applied forces and moments.

In this research, detailed information about linkages between adjacent links is unnecessary; therefore, the second method was chosen. Fig. 1 presents the simplified version of the examined Kawasaki RS010L robot and its structural model and Table 1 presents the Denavita-Hartenberga (D-H) notation parameters.

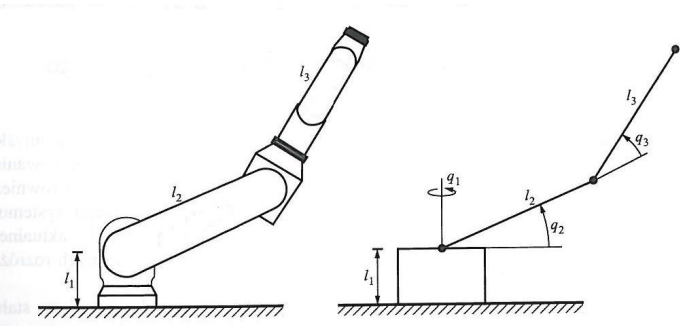

Fig. 1. The examined object and its structural model [5]

where:
l_1–l_3 – lengths of links,
q_1–q_3 – angular displacement in joints.

Table 1. D-H notation parameters of the model

i	Θ_i	d_i	a_i	α_i
1	q_1	l_1	0	$-\frac{\pi}{2}$
2	q_2	0	l_2	0
3	q_3	0	l_3	$-\frac{\pi}{2}$

The next step describes the dynamic relations of the servo drive, the schema of which is presented in Fig. 2. The set position of each joint is transferred to the PD controller and the output signal is then sent directly to the drive unit. There is a feedback in which the information from the sensor (usually an absolute encoder) is used to improve control quality. The model also contains three permanent magnet synchronous motors with DC/AC inverters and three PID controllers. Omitting the non-linear influence of mutual inductance, this system can be approximated by a linear mathematical model of a DC motor (2) [1, 9].

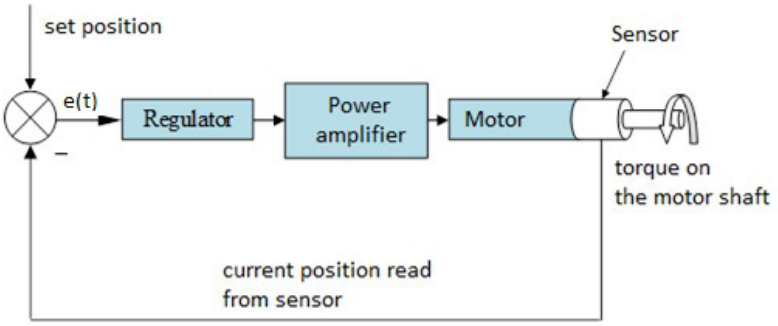

Fig. 2. Servo drive schema [14]

Presented equations (2) describing the DC model [14]:

$$\begin{cases} \dfrac{di_w}{dt} = -\dfrac{R_w i_w}{L_w} - \dfrac{k_e \omega_s}{L_w} + \dfrac{1}{L_w} U_z \\ \dfrac{d\omega_s}{dt} = -\dfrac{k_m i_w}{J} - \dfrac{B\omega_s}{J} - \dfrac{1}{J} M \end{cases} \tag{2}$$

where:
U_z – voltage feeding the motor rotor,
$-i_w$ – current in the motor windings,
R_w – equivalent impedance in the motor windings,
L_w – equivalent inductance in the motor windings,
E – electromotive force (as linear function of the rotor speed),
ω_w – angular speed of rotor,
B – viscous friction coefficient reduced to the motor shaft,
J – moment of inertia coefficient reduced to the motor shaft,
M – torque on the motor shaft,
k_e – electrical constant,
k_m – torque constant.

Equation (3) describing PD controller [14]:

$$U_z(t) = K_p e(t) + K_d \frac{d}{dt} e(t) \tag{3}$$

where:
K_p – proportional gain,
K_d – derivative gain,
$e(t)$ – error value.

The following equations (1–3) are linked together. First of all, displacement of the joint is connected with displacement of the rotor by the gear. Thus, the values of torque M and τ are also connected to one another with a certain ratio ($ratio_1$–$ratio_3$). According to Fig. 2, the output value of voltage from (3) is transferred to equation (2). The final mathematical model can be written as follows (4):

$$\dot{x}=\begin{cases}\dot{q}_1\\ \dot{q}_2\\ \dot{q}_3\\ (k_{m1}\cdot i_1-B\cdot\dot{q}_1)\cdot ratio_1-c_{112}\cdot\dot{q}_1\cdot\dot{q}_2-c_{113}\cdot\dot{q}_1\cdot\dot{q}_3\\ (k_{m2}\cdot i_2-B\cdot\dot{q}_1)\cdot ratio_2-c_{211}\cdot\dot{q}_1^{\,2}-c_{233}\cdot\dot{q}_3^{\,2}-c_{223}\cdot\dot{q}_2\cdot\dot{q}_3-\phi_2\\ (k_{m3}\cdot i_3-B\cdot\dot{q}_1)\cdot ratio_3-c_{311}\cdot\dot{q}_1^{\,2}-c_{322}\cdot\dot{q}_2^{\,2}-\phi_3\\ (Uz_1-R_w\cdot i_1-k_{e1}\cdot\dot{q}_1/ratio_1)/L_w\\ (Uz_2-R_w\cdot i_2-k_{e2}\cdot\dot{q}_2/ratio_2)/L_w\\ (Uz_3-R_w\cdot i_3-k_{e3}\cdot\dot{q}_3/ratio_3)/L_w\end{cases} \tag{4}$$

where

$$c_{112}=-[(2\cdot m_3\cdot l_2^{\,2}+0.5\cdot m_2\cdot l_2^{\,2}+2\cdot J_2)\cdot\sin(q_2)\cdot\cos(q_2)+$$
$$+m_3\cdot l_2\cdot l_3\cdot(\cos(q_2)\cdot\sin(q_2+q_3)+\sin(q_2)\cdot\cos(q_2+q_3))+$$
$$+(2\cdot J_3+0.5\cdot m_3\cdot l_3^{\,2})\cdot\cos(q_2+q_3)\cdot\sin(q_2+q_3)]$$

$$c_{113}=-[m_3\cdot l_2\cdot l_3\cdot\cos(q_2)\cdot\sin(q_2+q_3)+(2\cdot J_3+0.5\cdot m_3\cdot l_3^{\,2})\cdot\cos(q_2+q_3)\cdot\sin(q_2+q_3)]$$

$$c_{211}=0.5\cdot m_3\cdot l_2\cdot l_3\cdot(\sin(q_2)\cdot\cos(q_2+q_3)+\cos(q_2)\cdot\sin(q_2+q_3))+$$
$$+(m_3\cdot l_2^{\,2}+J_2+0.25\cdot m_2\cdot l_2^{\,2})\cdot\sin(q_2)\cdot\cos(q_2)+(J_3+0.25\cdot m_3\cdot l_3^{\,2})\cdot\sin(q_2+q_3)\cdot\cos(q_2+q_3)$$

$$c_{233}=-0.5\cdot m_3\cdot l_2\cdot l_3\cdot\sin(q_3)$$

$$c_{223}=-m_3\cdot l_2\cdot l_3\cdot\sin(q_3)$$

$$c_{311}=0.5\cdot m_3\cdot l_2\cdot l_3\cdot\cos(q_2)\cdot\sin(q_2+q_3)+(J_3+0.25\cdot m_3\cdot l_3^{\,2})\cdot\cos(q_2+q_3)\cdot\sin(q_2+q_3)$$

$$c_{322}=0.5\cdot m_3\cdot l_2\cdot l_3\cdot\sin(q_3)$$

$$\phi_2=(m_3\cdot l_2+0.5\cdot m_3\cdot l_2)\cdot\cos(q_2)+0.5\cdot m_3\cdot l_3\cdot\cos(q_2+q_3)$$

$$\phi_3=0.5\cdot m_3\cdot l_3\cdot\cos(q_2+q_3)$$

3. Assumptions and parameter identification

When the model has been constructed, the next step is to identify all constant values. In the case of the robot, a lot of information can be found in its documentation. However, some assumptions have been made. First of all, it was assumed that all links of the robot are long thin rods with a specific mass concentrated in its centre of gravity. Moreover, there is no information about the gear ratio of the robot's gears; therefore, this was determined through trial and error. The identified robot parameters are presented below:

$l_1 = 0.465m$, $l_2 = 0.77m$, $l_3 = 1.005m$, $m_1 = 62.8kg$, $m_2 = 54.7kg$, $m_3 = 62.1kg$,

$J_1 = 1.0Nm$, $J_2 = 2.5Nm$, $J_3 = 3.0Nm$, $ratio_1 = 63.15$, $ratio_2 = 58.54$, $ratio_1 = 57.14$

The same situation applies to the PD controller parameters, which are also values withheld by the company for purposes of industrial secrecy. Furthermore, to perform this research, it is crucial to find values of parameters which describe the robot motors. The RS010L industrial robot motors are AC Sanyo Denki R2AA13200LCP2S (Fig. 3), equipped with 17-bit SANMOTION PA035-017BC00S absolute sensors. Table 2 contains motor specification. It is very hard to determine the exact values of the torque on the motor shaft; therefore, the currents flowing through this engine are considered to be proportional to values of torque.

Table 2. Sanyo Denki R2AA13200LCP2S motor specification [16]

Power	2000 W
Rotation speed	2000 rpm
Electrical constant k_e	0.0337 V/rpm
Torque constant k_m	0.97 N*m/A
Rated current	35 A
Rated voltage	200 V
Rotor inductance R_w	0.0037 H
Rotor winding resistance L_w	0.22 Ω

Fig. 3. Applied motor with absolute encoder

In order to read the required performance parameters of the robot, it was necessary to activate the hidden service mode (Lv3) on Teach Pendant and to install additional software called "Data Storage" to the control cabinet. This module allows viewing these parameters on the Teach Pendant and to save them to an external device.

4. Measurement stand and research method

In order to verify the created model, the measurement stand shown in Fig. 4 was prepared.

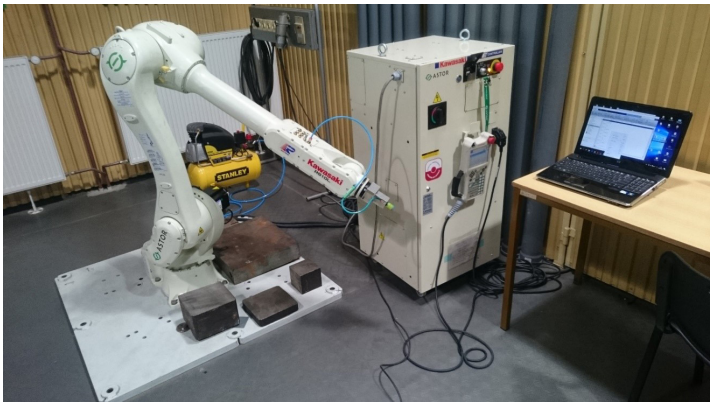

Fig. 4. Measurement stand for model verification

The measurement stand consists of a Kawasaki RS010L robot, a control cabinet E40F-A001, a Teach Pendant, a pendrive and a laptop with Matlab software containing the previously discussed simulation model. A series of measurements were made in several initial positions. These consisted of one slow and one quick transition of the manipulator between the starting point and another programmed position, changing the value of only one joint coordinate. As a result of this, it was possible to observe differences in the behaviour of the object under various operating conditions. Four movements were considered. The first three realised the movements of subsequent rotational pairs across a small range of motion. The result was the generation of torque τ_i, $i = 1, \ldots, 3$, where i represents sequent joints. Last "The final"? movement passed through the unstable equilibrium point using a third joint and as a result torque τ_{eq} was generated. External data such as angular displacement and angular velocity of joints as well as currents in the engines were recorded on an external medium – a pendrive. Angular displacements and velocities from measurements were entered into the mathematical model. The aim of the research was to compare the compliance of both input data (motion parameters) and output data (current values) from measurements and simulations. As an indicator of convergence of the obtained results, root-mean-square (RMS) was applied, which provides an estimate of the total error.

5. Results of model verification

Fig. 5 shows the starting positions of two selected robot's. The first of these (on the left) is specific because the link between the second and third swing pairs is arranged vertically. This also allows the robot's behaviour to be assessed for an unstable equilibrium position, i.e. when the deflected link is also arranged vertically.

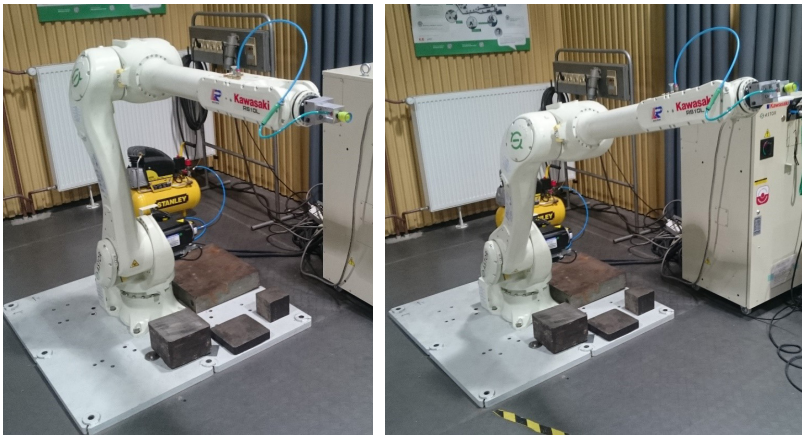

Fig. 5. Selected initial positions of robot (position 1 on left, position 2 on right)

The measurement results for the first position are shown below. In this case, the first rotational pair is moved by an angle of about 90 degrees. Fig. 6 presents the course of changes of this value using the data from the measurement and simulation. Slow movement of the manipulator is visible from seconds 1 to 10 and fast movement between seconds 10 and 12. The value of RMS for the first is 0.003 degrees, and for fast movement is 0.01 degrees. Fig. 7 shows the course of changes in the angular velocity of the joint.

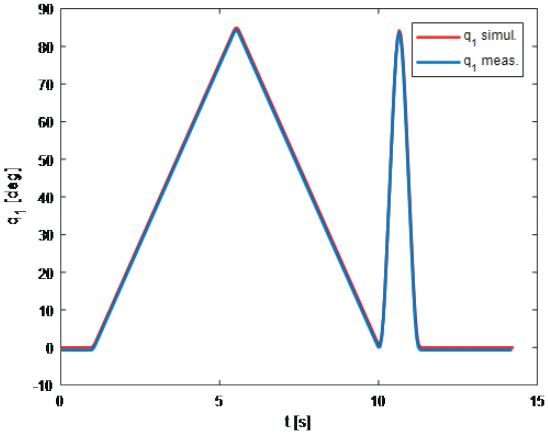

Fig. 6. The course of change of angular displacement in the first joint

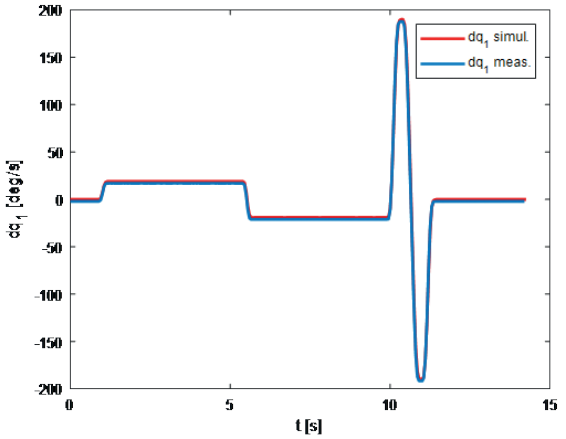

Fig. 7. The course of change of angular velocity in the first joint

The courses of change is convergent. The RMS value for the angular velocity for slow motion is 0.002 degrees per second, and for the fast speed, it is 0.03 degrees per second. It is worth noting that during slow motion, the rotating pair moved at a speed of around 15 degrees per second and during the rapid motion with its maximum speed of around 190 degrees per second. Fig. 8 shows the course of i_1 current changes in the motor driving the first rotational pair. There is a discrepancy of the current value in the slow movement of the manipulator; this may be due to the omission of the nonlinear influence of mutual inductance in the engine.

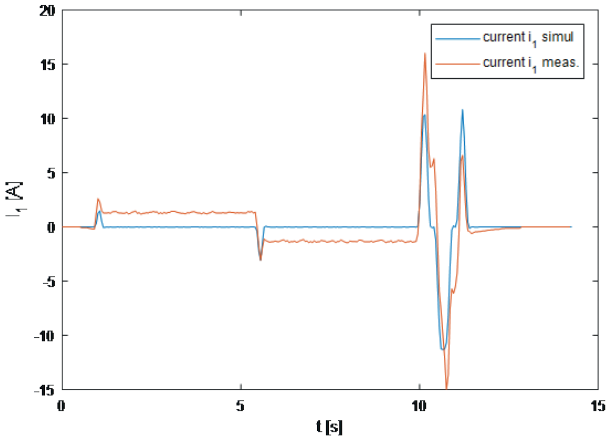

Fig. 8. The course of change of current value on first motor

Table 3 contains a complete list of the tests results. Each row contains information about the robot's position number, the generated torque and the analysed joint (in bracket). For example, "Pos. 1, $\tau_2(q_3)$" means that examination was performed in the first initial position

using the second joint and the motion parameters of the third joint and the current in its motor were analysed. The values of the RMS parameter designated separately for slow and fast motion are presented. For the second and third generated torque, two sets of solutions are shown because the second and third link are coupled. This means that if the third link moves (especially in fast movement), it will affect the second link under inertia force. It can be seen that during the fast movement, RMS values are larger by one order of magnitude. In the case of values of current, the model error is relatively large and increases with the increase of the speed of movement. This is due to the fact that the model contains simplified AC motors. A greater deviation of the measured parameters occurs in the second position, i.e. with an increased tilt of the second link of the manipulator.

Table 3. Complete list of results

	Angular displacement Slow motion [degrees]	Angular displacement Fast motion [degrees]	Angular velocity Slow motion [degrees per second]	Angular velocity Fast motion [degrees per second]	Motor current Slow motion [A]	Motor current Fast motion [A]
Pos. 1, $\tau_1(q_1)$	0.003	0.01	0.002	0.03	1.24	2.45
Pos. 1, $\tau_1(q_2)$	0.006	0.01	0.005	0.01	1.21	3.42
Pos. 1, $\tau_2(q_3)$	0.008	0.04	0.004	0.04	1.22	2.74
Pos. 1, $\tau_3(q_3)$	0.007	0.01	0.009	0.03	2.2	4.22
Pos. 1, $\tau_3(q_2)$	0.034	0.074	0.008	0.05	0.73	2.61
Pos. 1, $\tau_{eq}(q_3)$	0.008	0.09	0.01	0.07	2.71	4.21
Pos. 2, $\tau_1(q_1)$	0.009	0.02	0.01	0.03	1.34	4.1
Pos. 2, $\tau_2(q_2)$	0.007	0.17	0.019	0.14	2.63	4.11
Pos. 2, $\tau_2(q_3)$	0.03	0.32	0.034	0.17	1.77	3.9
Pos. 2, $\tau_3(q_2)$	0.017	0.06	0.03	0.26	1.32	1.98
Pos. 2, $\tau_3(q_3)$	0.008	0.11	0.02	0.13	3.89	4.76

6. Conclusions

The article presents a simplified dynamic model of a 6-axis industrial manipulator with a control system. It is limited to three kinematic pairs, as their size and weight significantly exceed the parameters of the gripper. In the next course of work, it would be worth to include a full-sized robot. It would also be necessary to change the form of the equations: take the integral term of the controller and create a full PID into the model. This will definitely

affect the quality of regulation. The values of currents from simulations and tests were not convergent. This is due to the fact that the model contains equations of DC motor dynamics and the tested object – AC motor dynamics. This is another direction that needs refinement. Another aspect is the fact that as a simplification, it is assumed that the moments of loading the motors are not considered directly. Currents value, passing through the motors, which are proportional to the value of this moment are determined. A separate measuring station should be prepared and an approximate dependence on the current value of the moment depending on the current flowing in the motor windings should be determined using the experimental method.

References

[1] Ahmad M., *High Performance AC Drives. Modelling Analysis and Control*, Springer 2010.

[2] Atkeson Ch.G., An Ch.H. and Hollerbach J.M., *Estimation of inertial parameters of manipulator loads and links*, International Journal of Robotics Research 1986, vol. 5, no. 3, 101–119.

[3] Ding L., Wu H., Yao Y., Yang Y, Dynamic Model Identification for 6-DOF Industrial Robots, Journal of Robotics Volume 2015, Article ID 471478.

[4] Gautier M. and Poignet P., *Extended Kalman filtering and weighted least squares dynamic identification of robot*, Control Engineering Practice, vol. 9, no. 12, pp. 1361–1372, 2001.

[5] Heimann B., Gerth W., Popp K. *Mechatronik: Komponenten – Methoden – Beispielen*, Hanser Verlag, Munich 2006.

[6] Jezierski E., *Dynamika robotów*, WNT, Warszawa 2006 (in Polish).

[7] Karaboga D., *An idea based on honey bee swarm for numerical optimization*, Tech. Rep. tr06, October 2005, Computer Engineering Department, Engineering Faculty, Erciyes University, 2005.

[8] Karaboga D. and Basturk B., *On the performance of artificial bee colony (ABC) algorithm*, Applied Soft Computing Journal 2008, vol. 8, no. 1, 687–697.

[9] Krykowski K., Piwowarczyk R., Radczuk C., *Poszerzenie zakresu prędkości silnika bezszczotkowego prądu stałego z magnesami trwałymi (PM BLDC) przez zastosowanie przekształtnika podwyższającego BOOST*, Materiały Krajowej Konferencji Naukowej SENE, Łódź 2007, 259–266 (in Polish).

[10] Liu Y., Li G.-X., Xia D., Xu W.-F., *Identifying dynamic parameters of a space robot based on improved genetic algorithm*, Journal of Harbin Institute of Technology 2010, vol. 42, no. 11, pp. 1734–1739.

[11] Morecki A., Knapczyk J., Kędzior K., *Teoria mechanizmów i manipulatorów*, WNT, Warszawa 2002 (in Polish).

[12] Sánchez-Sánchez P., Arteaga-Pérez M.A., *Simplied Methodology for Obtaining the Dynamic Model of Robot Manipulators, International Journal of Advanced Robotic Systems*, DOI: 10.5772/51305.

[13] Spong M.W., Hutchinson S., Vidyasagar M., *Robot Dynamics and Control. Second Edition*, John Wiley & Sons, Inc., Canada 2004.
[14] Szkodny T., *Dynamika robotów przemysłowych*, Wyd. Politechniki Śląskiej, Gliwice 2013 (in Polish).
[15] Zakharov A., Halasz S., *Parameter identification of a robot arm using genetic*, Periodica Polytechnica Ser. El. Eng. 2001, vol. 45, no. 3–4, 195–209.
[16] Kawasaki [online] https://robotics.kawasaki.com/en1/products/robots/small-medium-payloads/RS010L/ (access: 26.10.2018).